Biotribology 18 (2019) 100092

Contents lists available at ScienceDirect

Biotribology

journal homepage: www.elsevier.com/locate/biotri

# Responsive polysaccharide-grafted surfaces for biotribological applications

Clementine Pradal[a], Gleb E. Yakubov[a,1], Martin A.K. Williams[b], Michael A. McGuckin[c,d], Jason R. Stokes[a,*]

[a] School of Chemical Engineering, The University of Queensland, St Lucia, Queensland, Australia
[b] Institute of Fundamental Sciences, Massey University, Palmerston North, New Zealand
[c] Mater Research Institute, Translational Research Institute, The University of Queensland, Woolloongabba, Queensland, Australia
[d] Faculty of Medicine, Dentistry and Health Sciences, The University of Melbourne, Victoria, Australia

ARTICLE INFO

*Keywords:*
Biotribology
Polysaccharide lubrication
MTM-2
QCM-D
Ionic strength
Pectin

ABSTRACT

The elucidation of biolubrication mechanisms and the design of artificial biotribological contacts requires the development of model surfaces that can help to tease out the cues that govern friction in biological systems. Polysaccharides provide an interesting option as a biotribological mimic due to their similarity with the glycosylated molecules present at biointerfaces. Here, pectin was successfully covalently grafted at its reducing end to a polydimethylsiloxane (PDMS) surface via a reductive amination reaction. This method enabled the formation of a wear resistant pectin layer that provided enhanced boundary lubrication compared to adsorbed pectin. Pectins with different degrees of methylesterification and blockiness were exposed to salt solutions of varying ionic strength and displayed responsiveness to solvent conditions. Exposure of the grafted pectin layers to solutions of between 1 and 200 mM NaCl resulted in a decrease in boundary friction and an increase in the hydration and swelling of the pectin layer to varying degrees depending on the charge density of the pectin, showing the potential to tune the conformation and friction of the layer using the pectin architecture and environmental cues. The robust and responsive nature of these new pectin grafted surfaces makes them an effective mimic of biotribological interfaces and provides a powerful tool to study the intricate mechanisms involved in the biolubrication phenomenon.

## 1. Introduction

Biotribology is a ubiquitous phenomenon in the human body and is essential to a multitude of biological functions such as joint movement, blinking or swallowing. Deficiencies in lubrication between biological substrates have a major impact on the quality of life for people with osteoarthritis, dry-eye or dry-mouth syndrome [1–3]. The mechanisms of biolubrication still remain to be fully elucidated, mostly due to the difficulty of measuring lubrication in vivo and the lack of relevant in vitro models. Despite the absence of a full picture, it is known that biolubricating contacts share key features that can be harnessed in biomimetic strategies. The presence of glycosaminoglycans or glycosylated proteins, such as hyaluronic acid (HA), aggrecan and lubricin for cartilage [4,5] or mucins for oral surfaces [6,7], is thought to be paramount to the lubricating performance of the biological interfaces. The strong interactions between the sugar moieties and the water molecules enables the water to remain “trapped” in the contact, rather than be squeezed out when the surfaces are pushed towards each other, thus ensuring that a hydrated layer is maintained in the contact. Additionally, the brush-like architecture of the glycosylated macromolecules is an effective way to reduce friction in the boundary regime: when two surfaces covered with neutral polymer brushes come in contact at low to moderate compression, it is entropically more favourable for the brushes to compress within themselves than to interpenetrate with the brushes on the opposite surface, thus decreasing the interaction between the surfaces [8–10]. When the brushes are charged, as is the case for mucins, lubricin and aggrecan, the additional effects of the osmotic pressure created by trapped counterions and the lubricating effect of the hydration shells around the charged monomers, called the hydration lubrication effect, improves the lubrication properties of the brushes at high loads [11–13]. The charged nature of the brushes also renders the lubricating films responsive to solvent changes: for instance the mucins present in the salivary film have been found to collapse or swell depending on the ionic strength, with potential consequences on oral health or sensory perception [14,15].

Current methods to study biolubrication or emulate the low friction

* Corresponding author.
*E-mail address:* jason.stokes@uq.edu.au (J.R. Stokes).
[1] Current Location: School of Biosciences, University of Nottingham, Sutton Bonington, Leicestershire, UK.

https://doi.org/10.1016/j.biotri.2019.100092
Received 4 February 2019; Received in revised form 26 March 2019; Accepted 30 March 2019
Available online 01 April 2019

coefficients encountered in the body usually involve forming lubricating layers from artificial polymers, or adsorbing lubricating biomolecules (e.g. mucin, hyaluronic acid) or fluids (e.g. saliva, synovial fluid) onto surfaces. Neutral or charged polymer brushes have been the focus of a high number of studies due to their resemblance to the brush-like structure of glycosylated proteins and have been used to identify the roles of brush side chain length and density, pH, salts and solvent viscosity on the lubrication properties of those brushes. Examples of such polymer brushes include adsorbed poly(L-lysine)-*graft*-poly(ethylene) glycol (PLL-PEG) [16–23] and poly(L-lysine)-*graft*-dextran (PLL-Dex) brushes [20,24,25] and covalently grafted polyzwitterionic poly [2-(methacryloyloxy) ethyl phosphorylcholine)], (pMPC) brushes [26–28]. The later have shown promising results in terms of attaining friction coefficients close to the ones found in the body thanks to the high level of hydration of the brushes [29]. Using biomolecules encountered in the lubricating fluids, such as mucins [7,30–33] or lubricin [5,34], adsorbed onto surfaces as in vitro models presents the advantage of offering a better match to the biochemical make-up of the native biotribological contacts. However, not all biomolecules are commercially available in the native state and require purification from biological fluids [35], which limits their application as biomimetic models. Additionally, using adsorption to coat the surfaces can result in poor wear resistance as the adsorbed layer can be damaged or removed under rubbing conditions due to shear and pull-off forces. Few studies have investigated the possibility of grafting biomolecules to surfaces for lubrication applications and most of these have focused on HA. Chemisorbed [36] and peptide-bound [37] HA has shown an enhancement in lubrication compared to adsorbed HA, while covalent binding of HA to the surface has also been used to highlight its role in wear resistance [38–40]. In these examples, the grafting to the surface has been carried out along the whole polysaccharide chain rather than at a single end-point, thus constraining its conformation and potentially limiting its lubricating ability and responsiveness. Dextran has been grafted at a terminal residue, however, bridging issues between the surfaces caused high friction at high loads [41,42].

Inspired by nature's use of charged glycosylated proteins and polysaccharides in biological contacts, we propose a new type of biotribological model surface that consists of pectin molecules grafted at one extremity onto polydimethylsiloxane (PDMS) using reductive amination. Pectin is a biocompatible, non-toxic anionic polysaccharide extracted from plant cell walls, and is composed of a main backbone of 1,4 linked D-galacturonic acid units, either present as carboxylic acids or in a methylesterified form, with a small proportion of interspaced rhamnogalacturonan I (RG I) and rhamnogalacturonan II (RG II) [43]. The amount of methylesterified units and the distribution of the methylesterified groups can be chemically or enzymatically modified to provide a highly tunable architecture, where the global and local charge density can be controlled. Pectin adsorbs onto hydrophobic surfaces and forms a lubricating film [44] but this adsorbed layer is expected to suffer from lack of resistance to wear. Here, we anticipate that the covalent grafting of pectin will provide a robust lubricating polyelectrolyte layer with a biochemical composition relevant to biotribological applications. Additionally, it is expected that the grafted pectin will display a responsive conformation that swells or contracts upon changes in solvent conditions, thus forming a mimic of biological surfaces and providing a useful tool to understand the mechanisms of biolubrication.

## 2. Materials and Methods

### 2.1. Materials

Custom made pectins were supplied by CP Kelco. Systematic variation in the degree of methylesterification (DM) of the galacturonic acid units and the degree of blockiness (DB) [45] was achieved via enzymatic modification of the same 'mother' pectin extracted from citrus. The composition of the three pectins used in this study is summarised in Table 1. Two of the pectins have a low DM, meaning that a small proportion of the galacturonic acid groups are in the methylester form. One of the pectins is "blocky", meaning that a high proportion of the methylesterified units are grouped together, as opposed to randomly distributed along the molecule.

**Table 1**
Composition of the pectins used in this study.

| Pectin sample | Description | Charge distribution | | Pectin molecular weight $M_n$ (g/mol)[a] |
|---|---|---|---|---|
| | | % DM | % DB | |
| LM-B | Low DM, blocky | 31 | 70 | 200,000 |
| LM-R | Low DM, random | 33 | 46 | 230,000 |
| HM-R | High DM, random | 69 | 17 | 220,000 |

[a] Determined using an Agilent 1260 Infinity aqueous Gel Permeation Chromatography (GPC) system equipped with a refractive index detector. Solutions containing 2 mg/ml of pectin in water were run in a PL-Aquagel-OH Mixed-M 8 µm column with water containing 0.2 g/L of $NaN_3$ as the mobile phase, with a flow rate of 1 ml/min at 30 °C.

(3-Aminopropyl)trimethoxysilane (APTMS), sodium cyanoborohydride, sodium dodecyl sulfate (SDS) were obtained from Sigma-Aldrich. Sodium Chloride was obtained from Ajax Finechem and the PDMS base and curing agent kit (Sylguard 184), were obtained from Dow Corning.

Unless otherwise specified, the water used in this study was reverse osmosis (RO) treated water with a resistivity of 18.2 MΩ cm (Sartorius Stedim) and all solutions were made using this RO treated water. The pH of the water was 5.8.

When using a lubricant other than water (i.e. salt solutions or pectin solutions), the pH was checked and adjusted to match the pH of the RO treated water at 5.8 using 0.1 M NaOH and 0.1 M HCl to ensure that all measurements were performed at a comparable pH. The typical pKa of pectin is in the range of 3.5–5 [46] therefore the pectin molecules are negatively charged at the pH used here.

### 2.2. Covalent grafting of polysaccharides onto the surfaces

PDMS ball and disc tribopairs were fabricated as described in [47], by mixing the base and curing agent in a ratio of 10:1, casting the mixture in specifically designed moulds and curing overnight at 60 °C. After demoulding and cutting to size, the tribopairs were thoroughly rinsed and sonicated in isopropanol then in water to remove any uncrosslinked material. Further cleaning was performed using sonication in 1% SDS then in water to remove any other contaminant. The surfaces were then characterised by measuring their Stribeck curve in water (see method below) in order to select tribopairs with similar friction coefficient. This ensured that any differences in the friction coefficient observed post-grafting were only due to the grafting process rather than to intrinsic differences between the tribopairs.

The surfaces were thoroughly dried using nitrogen, then placed in an oxygen plasma cleaner (Harrick Plasma, NY) for 1 min. After plasma treatment, the tribopair was immersed in a solution of 10% APTMS in ethanol with gentle mixing on an orbital shaker for 2 h at room temperature. The surfaces were then thoroughly rinsed with ethanol, dried with nitrogen and placed in an 80 °C oven for 1 h to yield aminated tribopairs. The use of APTMS rather than the more conventionally used 3-Aminopropyl)triethoxysilane (APTES) was found to be essential. Preliminary experiments using APTES in the grafting process did not lead to a significant reduction in the friction coefficient, thus indicating a poor grafting outcome compared to APTMS.

The aminated tribopairs were immersed in a solution of 10 mg/ml pectin and 1 mg/ml sodium cyanoborohydride in water and placed on an orbital shaker for four days at room temperature (Fig. 1). After the

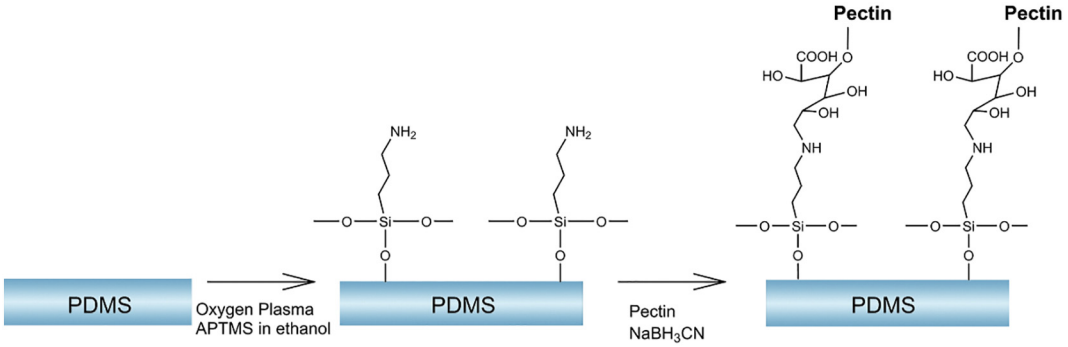


**Fig. 1.** Reaction Scheme for the covalent grafting of pectin onto PDMS via reductive amination.

reductive amination reaction, the tribopairs were sonicated in 1% SDS followed by sonication in water to remove any unreacted pectin. The samples were then stored in water. At least two tribopairs were functionalised by this method and characterised for each pectin. The friction coefficient obtained for each replicate was found to be reproducible and the grafted tribopairs were stable for several months when stored in water. Additional control tribopairs were fabricated by aminating some tribopairs according to the method above and keeping them in either water for 4 days or in pectin (without any reducing agent) for 4 days. These tribopairs were also sonicated in 1% SDS followed by sonication in water to remove any unreacted materials. These controls were used to determine whether the aminating process had an impact on the friction coefficient and whether pectin could spontaneously form SDS wash resistant electrostatic interactions with the aminated surfaces that would influence the friction coefficient.

### 2.3. Surface characterization of the grafted pectin layers

X-Ray Photoelectron Microscopy was performed on a Kratos Axis ULTRA X-ray Photoelectron Spectrometer (Kratos Analytical, UK) incorporating a 165 mm hemispherical electron energy analyser. The incident radiation was monochromatic Al Kα X-rays (1486.6 eV) at 150 W (15 kV, 10 mA) and photoelectron data were collected at a take-off angle of θ = 90°. Survey (wide) scans were taken at an analyser pass energy of 160 eV and multiplex (narrow) high resolution scans were taken for carbon (C 1s) at 20 eV. Atomic concentrations were determined and curve fitting carried out using the CasaXPS version 2.3.14 software and a linear baseline with Kratos library Relative Sensitivity Factors (RSFs). Charge correction was applied by setting the observed value of C 1s to be 284.8 eV [48]. To avoid degassing issues when using the thick PDMS samples from the tribopairs, thinner PDMS fragments were produced for the XPS experiments by casting the PDMS mixture into petri dishes to obtain ~1–2 mm thick PDMS sheets, that were then cut into 1 cm × 1 cm square fragments and functionalised with pectin in the same manner as described above.

Contact angle was measured on an OCA20 system (Dataphysics, Germany). 10 µl drops of water were deposited on the PDMS disc using an automated syringe and photos were taken with a high resolution camera. The images were processed using the SCA20 software to extract the advancing contact angle. For each sample, the average and standard deviation of 10 contact angle measurements taken from 10 individual drops deposited at different locations on the PDMS disc is reported. One way ANOVA tests were performed using the software GraphPad Prism 7 (CA) to determine the significance of the differences observed between the samples.

### 2.4. Tribology

The tribological properties of the pectin grafted tribopairs were characterised using a ball-on-disc tribometer (MTM2, PCS Instruments Ltd., UK). Controls with unmodified PDMS and pectin adsorbed onto the PDMS from a 0.1% (w/v) solution were also used. The use of compliant contacts enables the experiments to match more closely the pressure conditions typically encountered in the body [47]. The ball and disc were prepared following the method described above have the following characteristics: the ball has a radius of 0.95 cm, the disc radius is 2.3 cm and the Young's modulus of both disc and ball is 2.4 MPa [47]. Both the ball and disc were functionalised with pectin.

For the Stribeck curves, the friction force $F_f$ was measured as a function of the entrainment speed, $U$, defined as the average surface speed of the ball and disc, $U = (U_{ball} + U_{disc})/2$, over the range of 1 to 1000 mm/s in logarithmic intervals. One measurement consists of five repetitions of alternately descending and ascending entrainment speeds. Measurements were performed in triplicates at 35 °C. A temperature of 35 °C was chosen to mimic the temperature of biological interfaces like oral surfaces [49] or the ocular surface [50,51]. The average and standard deviation of the three repeats is reported. For all tests, a normal load ($W$) of 1 N was applied on the ball and a slide-to-roll ratio (SRR) of 50% was used to impart both sliding and rolling motion, where $SRR\ (\%) = 100|U_{ball} - U_{disc}|/U$. The friction coefficient ($\mu$) is calculated as the friction force divided by applied load ($\mu = F_f/W$).

For the load ramp curves, the friction force was measured at a speed of 5 mm/s, a SRR of 50% and at varying normal loads between 0.5 N and 8 N (the maximum load that can be reached using the set up) at 35 °C. Each load was maintained for 2 min before being ramped up to the next load value, starting from 0.5 N. The average friction force at equilibrium for each load was used in the analysis. The experiment was performed in duplicates, the average and standard deviation of the duplicates is reported.

To measure the response to changes in the ionic strength, the friction force was measured for various salt concentrations at a speed of 5 mm/s, a SRR of 50% and a constant 1 N normal load for 2 min at 35 °C. The average friction force at equilibrium for each salt concentration was used in the analysis. The average and standard deviation of three repeats is reported.

### 2.5. Ellipsometry

Ellipsometry was used to measure the dry thickness of the grafted pectin films using a M-2000 V spectroscopic ellipsometer (J.A. Woollam, NE) at 55, 60, 65, 70 and 75° at wavelengths between 370 and 1000 nm. The measurements were performed on a PDMS coated quartz crystal microbalance with dissipation monitoring (QCM-D) disc (coating method described in [14], resulting in a PDMS layer of ~5–6 nm, also characterised by ellipsometry) and grafted with the pectin layer as described above. The pectin layer thickness was obtained using the CompleteEASE software (version 5.1, J.A. Woollam) and fitting a Cauchy layer [52] on top of the PDMS layer. Due to the thin nature of the films, the Cauchy parameters were fixed (A = 1.50 [53], B = 0.01 and C = 0) and only the thickness of the pectin layer

was fitted. At least two separate QCM-D discs were functionalised and characterised for each type of pectin.

### 2.6. QCM-D

The changes in the grafted pectin layer upon variations of the solvent conditions were followed using a QCM-D E1 system (Q-Sense, Biolin Scientific, Sweden). Gold QCM-D sensors with a fundamental resonance frequency of 4.95 MHz (International Crystal Manufacturing, OK) were coated with PDMS to mimic the surfaces used in the tribological contact according to the procedure described my Macakova et al. [14]. Pectin was then grafted onto the PDMS coated QCM-D sensors using the same method as described above. Changes in the resonance frequency and dissipation of the oscillation energy of the piezoelectric quartz resonator were monitored overtime. A flow rate of 150 µl/min, controlled by a peristatic pump was used and the temperature was set to 35 °C. To ensure that no physisorbed contaminants were present on the surface, several washes with 1% SDS were performed, until the baselines before and after the washing step were identical. To assess the response to changes in ionic strength of the grafted pectin layers, the baseline was first recorded in water, then the salt solution was introduced into the QCM-D cell and left to equilibrate for 8 min before returning to pure water. The changes in the thickness and viscoelastic properties of the film upon addition of salt were modelled in Excel using a Voigt viscolelastic model [42].

## 3. Results

### 3.1. Formation of a lubricating and robust grafted pectin layer

#### 3.1.1. Characterisation of the grafted surfaces

We first focus on one type of pectin, pectin LM-B, and assess its grafting outcome as well as its lubrication properties when covalently tethered to the surface. The successful grafting of pectin onto PDMS was evaluated using XPS C1s narrow scans. Fig. 2A shows the C1s narrow scan for the aminated PDMS. The data was fitted using two peaks: the main peak at 284.8 eV corresponds to the C—H, C—C and C—Si bonds while the second peak at 286.1 eV is characteristic of the C—O and C—N bonds [54]. In the spectra of PDMS grafted with pectin in Fig. 2B, additional peaks are present at 286.8 and 288.3 eV, which are attributed to the acetal and the ester/carboxylic acid functional groups of pectin respectively [55,56]. Since the substrates had been thoroughly washed to remove any adsorbed pectin, the presence of these two additional peaks on the substrate confirms that successful grafting of pectin onto the PDMS.

The grafting reaction was found to modify the static contact angle of water on the substrate. The angle significantly decreased ($p < .001$), from 107 ± 3° for the unmodified PDMS to 69 ± 2° for the grafted LM-B pectin. To ensure that this transformation to a hydrophilic surface was not solely due to the PDMS amination reaction, the contact angle of a control PDMS sample functionalised with APTMS and stored in water for the same duration as the duration of the grafting reaction was measured. The contact angle for this surface was 98 ± 3°, which is significantly lower than unmodified PDMS (9°, $p < .001$) and significantly higher (29°, $p < .001$) than the pectin grafted surface, suggesting the grafted pectin renders the PDMS surface hydrophilic.

The grafting density $\sigma$ of the pectin is estimated using the pectin molecular weight obtained by GPC and the dry thickness ($d$) obtained by ellipsometry: $d = (4 \pm 1)$ nm for LM-B pectin, which are interrelated through the formula [57]: $\sigma = \frac{d\rho N_A}{M_n}$, where ρ is the density of pectin (1.51 g/cm$^3$ [58]), $N_A$ is the Avogadro number and $M_n$ is the number-averaged molecular weight of pectin. We obtain a grafting density of 0.02 pectin chains/nm$^2$. In order to assess the conformation of the grafted pectin on the surface when placed in water, the grafting density needs to be compared to the size of hydrated pectin molecules.

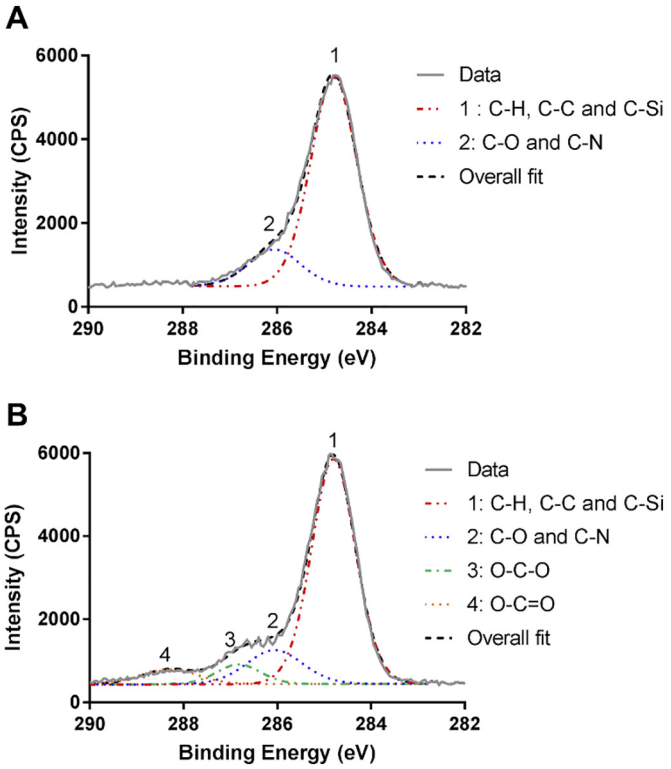


**Fig. 2.** C1s XPS scans of aminated PDMS (A) and PDMS grafted with LM-B pectin (B).The grey continuous line represents the data, the numbered coloured dotted and dashed lines represent the fit to the various carbon species and the dashed black line is the overall fit.

A rough minimum size of a pectin chain in solution is estimated using the equivalent Flory radius ($R_F$) [59] given by $R_F \sim aN^n$, where $a$ is the characteristic dimension of a galacturonic acid monomer, taken here as 0.45 nm [60], $N$ is the number of repeating units in the polymer and n is dependent on polymer conformation and equal to 0.6 for a swollen coil [61]. Assuming that pectin is in a swollen coil conformation in water or in the salt solutions used in this study, an estimate for $R_F = 29$ nm is obtained for pectin LM-B. This size is likely an underestimation due to pectin being a relatively rigid molecule, but using this size estimate to assess the so-called reduced grafting density allows the conformation to be already estimated as that of a brush (increases in the actual size will only strengthen this conclusion). Specifically, the reduced grafting density $\Sigma = \sigma\pi R_F^2$ represents the number of chains that occupy the area that a free polymer chain would occupy in the same experimental conditions and reflects the mushroom or brush-like nature of the grafted polymer chains [62]. For $\Sigma < 1$, the chains are in a mushroom conformation. For $\Sigma > 1$, the chains are stretched away from the surface in a brush like conformation and $\Sigma \approx 1$ corresponds to the mushroom to brush transition. Here, we find that $\Sigma > 1$ for the grafted pectin, which is an indication of a brush conformation.

#### 3.1.2. Tribological performance of the grafted pectin

The tribological performance of the LM-B pectin grafted surfaces was first assessed using a Stribeck curve that shows the dependence of the friction coefficient on the entrainment speed. Fig. 3 shows the Stribeck curve for LM-B pectin-grafted PDMS surfaces with water as the lubricant. For comparison, we include results for the unmodified PDMS surfaces lubricated with water or 0.1% (w/v) pectin LM-B, whereby pectin physically adsorbs from solution to the PDMS surface.

The grafted pectin provides the largest enhancement to lubrication, reducing the friction coefficient to $\mu_b \sim 0.6$ in the boundary regime, less than half the boundary friction coefficient value for unmodified PDMS ($\mu_b \sim 1.4$) lubricated by water. In comparison, unmodified PDMS

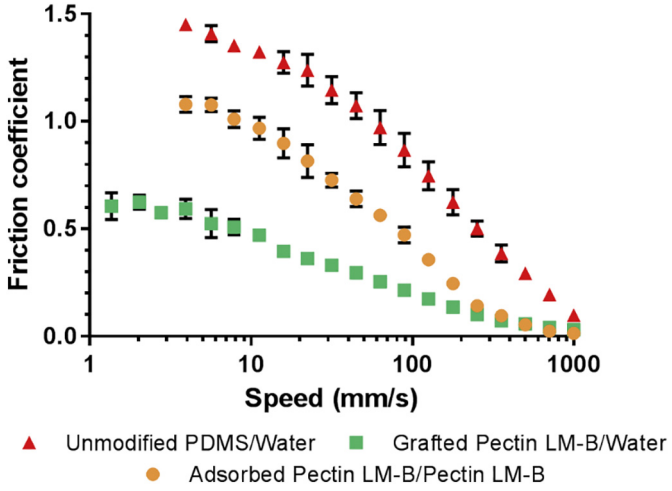


**Fig. 3.** Stribeck curves for the grafted LM-B pectin surface compared to hydrophobic PDMS and adsorbed pectin LM-B at 35 °C, for a normal load of 1 N. The legend refers to "surface"/"lubricant".

lubricated by an adsorbed layer of pectin LM-B only decreases the friction in the boundary regime to $\mu_b \sim 1.1$ and requires to have some dissolved pectin in the lubricant to replenish the adsorbed pectin layer: when the pectin solution is replaced by water, the friction coefficient of the adsorbed pectin increases to that of the unmodified PDMS ($\mu_b \sim 1.4$) in water due to desorption of the pectin layer (supplementary fig. S1). Additional controls showed that the decrease in friction observed for grafted pectin was not due to the amination reaction itself nor by SDS wash resistant electrostatic interactions between pectin and the amine groups on the aminated PDMS (supplementary fig. S2).

### 3.1.3. Wear resistance

To test the wear resistance of the grafted pectin layer, the grafted surfaces were subject to increasing loads at low speed (boundary regime). Wear resistance is important to ensure the stability of the surface upon exposure to high loads and enable the use of the grafted surfaces as biotribological models. Fig. 4 shows the friction force response of various surface/lubricant combinations at increasing loads at a constant entrainment speed of 5 mm/s. Grafted LM-B pectin in water retains the lowest friction force for all loads tested. As a comparison, adsorbed LM-B pectin yields a more moderate reduction in friction compared to unmodified PDMS and this only holds when dissolved pectin is also present in the lubricant. If the pectin lubricant is replaced by water, the adsorbed pectin wears off and the friction force returns to a similar level to unmodified PDMS in water. This result shows that covalently grafting pectin to the surface enables pectin to form a robust lubricating layer that does not require additional lubricant to reduce friction. This result can also be interpreted in terms of wear distance: each point on the graph in Fig. 4 corresponds to 2 min of testing. Knowing the speed of the disc (6.27 mm/s) and the wear track circumference (144.5 mm), we can calculate the distance travelled during each 2 min test: 752 mm. Since all the loads are tested consecutively, the wear distance cumulates as the load increases. When all the loads have been tested, the total cumulated wear distance is 7.52 m. Of all the surface/lubricant tested, the grafted pectin in water is the one that maintains the lowest friction through the whole distance tested and the friction does not jump to the values obtained for bare PDMS, showing that the grafted pectin stays on the surface (supplementary Fig. S3).

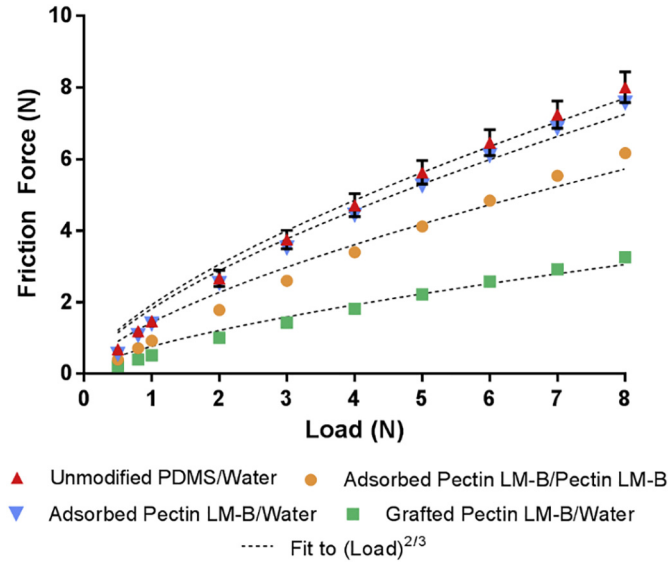


**Fig. 4.** Measured friction force versus applied load for various surface/lubricant systems at a constant speed of 5 mm/s.

As was previously observed by Stokes et al. [44] for the adsorbed polysaccharides, the friction force $F$ scales with the load as $F \sim W^{2/3}$. This dependency originates from the relationship $F = \tau_i A$ with $A$ the contact area and $\tau_i$ the interfacial shear strength between the surfaces. The contact area can be obtained from the Hertz equation that gives the true contact area for a circular contact: $A = \pi\left(\frac{3WR}{4E'}\right)^{2/3}$ with $W$ the applied load, $R$ the radius of the ball ($9.5{\cdot}10^{-3}$ m) and $E'$ the reduced Young's modulus of the tribopair (1.6 MPa).

The friction vs. load data were fitted using the expression $F = 8.5{\cdot}10^{-6}{\cdot}\tau_i{\cdot}W^{2/3}$ (see dashed lines in Fig. 4) which enables evaluating the value of the interfacial shear strength. We find that the adsorbed pectin modifies the interfacial shear strength between the surfaces, lowering it from 0.23 MPa for the PDMS/water system to 0.17 MPa for the adsorbed pectin/pectin system in the present study. The grafted pectin lowers the interfacial shear strength even further down to 0.09 MPa.

### 3.2. Influence of ionic strength and pectin architecture on the friction and swelling of grafted pectin

Fig. 5 shows the changes observed in the Stribeck curve of unmodified PDMS and the three grafted pectins with different molecular architectures (Table 1) upon exposure to 100 mM NaCl. The increased

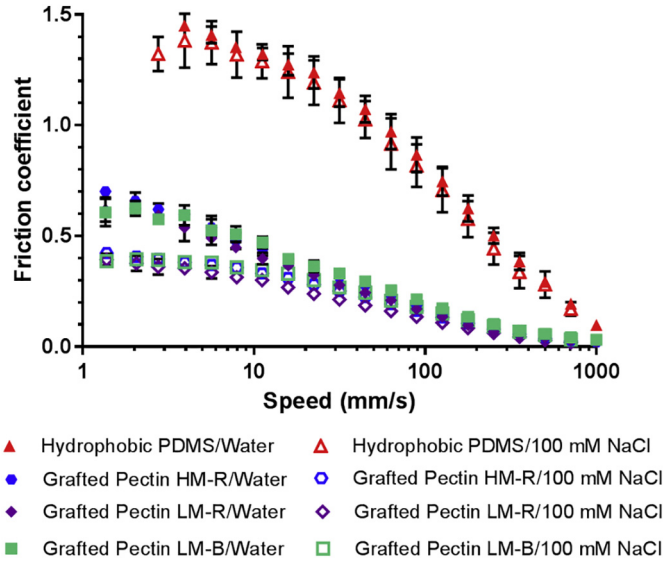


**Fig. 5.** Influence of ionic strength on the friction coefficient of unmodified PDMS and the three grafted pectins tribopairs at 35 °C, for a normal load of 1 N. The legend refers to "surface"/"lubricant".

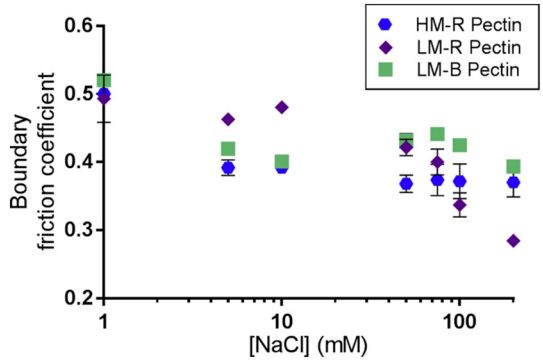


**Fig. 6.** Influence of ionic strength and pectin architecture on the boundary friction coefficient measured at 5 mm/s, 35 °C, for a normal load of 1 N.

ionic strength has little impact on friction for unmodified PDMS. However, it leads to a marked decrease in the boundary friction for the grafted pectin from $\mu_b \sim 0.6$ to $\mu_b \sim 0.4$. Pectin architecture is expected to influence the responsiveness to changes in ionic strength due to the differences in global and local charge density of the different pectins. Pectin LM-R and HM-R were grafted to the PDMS substrate using the same protocol as for LM-B, yielding a similar grafting density (Supplementary table 1). Fig. 6 shows the boundary friction coefficient obtained for grafted LM-B, LM-R and HM-R pectins at various salt concentrations. Generally the boundary friction coefficient decreases with increasing ionic strength, however some differences are observed for the three pectins. HM-R pectin shows the highest decrease in friction for low ionic strengths (5–50 mM), however this effect tapers off above 75 mM where the friction coefficient reaches a plateau. LM-R pectin shows a moderate decrease in friction at low ionic strength but unlike pectin HM-R, the friction coefficient continues to decrease at higher ionic strengths. Pectin LM-B shows a decrease in friction coefficient over the whole range of ionic strength studied but it has the highest friction coefficient of the three pectins above 50 mM NaCl.

QCM-D was used to probe the changes in layer thickness and layer viscoelasticity to aid corroborating the mechanisms responsible for the friction behaviour observed in the grafted pectin layers in response to the salt environment. The raw QCM data for pectin LM-B (Fig. 7) shows that when the grafted pectin comes in contact with a salt solution, the resonance frequency (3rd, 5th, 7th and 9th harmonic are shown) decreases and the dissipation increases to varying degrees depending on the type of pectin and the ionic strength. These changes are reversible and the pectin layer returns to its initial condition when the salt solution replaced back with water. Similar behaviour (as shown in Fig. 7 for LM-B) is observed for the other two pectins (Supplementary fig. S4).

The decrease in frequency observed for the grafted pectin upon addition of salt is indicative of an increase in wet mass of the pectin layer, which is consistent with swelling of the pectin layer due to penetration of hydrated ions. The dissipation of the pectin layer increases upon increase in the ionic strength, showing an increase in the viscoelastic character of the layer. Both properties are consistent with

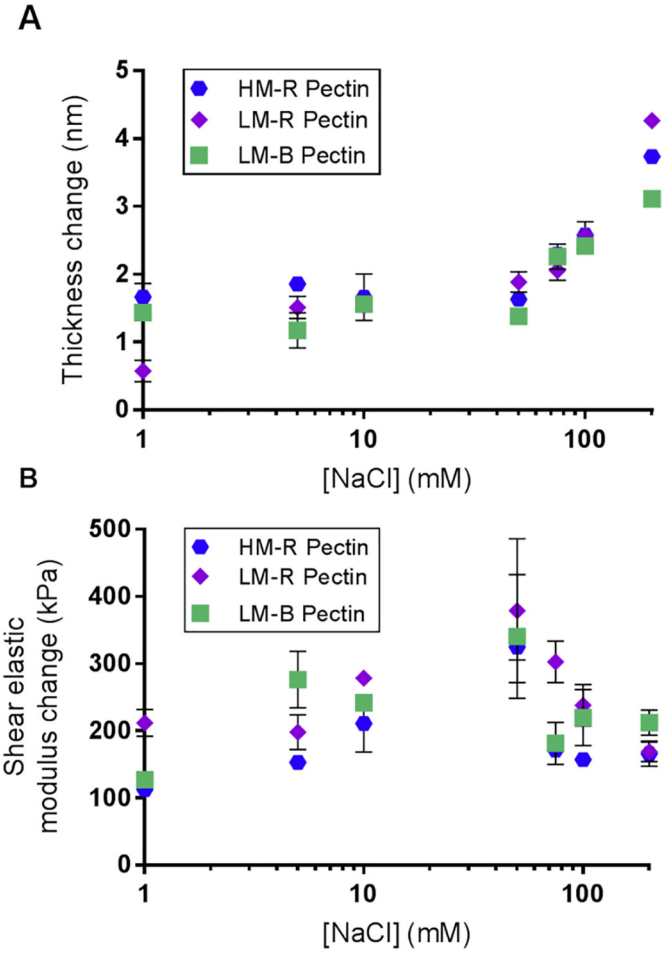


**Fig. 8.** (A) Grafted pectin layer thickness changes upon addition of salt solutions at varying concentrations. (B) Grafted pectin layer elastic modulus changes upon addition of salt solutions at varying concentrations.

hydration and swelling of the pectin layer in salt compared to the pure water conditions. The peaks observed in the dissipation curves soon after the solvent is exchanged in some of the curves are due to a gradient in salt concentration: the pectin layer expands as the salt concentration initially increases after coming into contact with the surface of the layer before contracting again once the equilibrium salt concentration is reached throughout. Conversely, the changes in frequency are smooth, demonstrating that the changes in wet mass are a more gradual process.

Fig. 8A summarises the changes in pectin thickness observed for the three pectins upon addition of salt in reference to the thickness in water. At low salt concentration (1 mM, 5 mM NaCl), HM-R pectin shows the largest increase in the thickness of the pectin layer, while at 200 mM NaCl pectin LM-R undergoes the largest change in thickness.

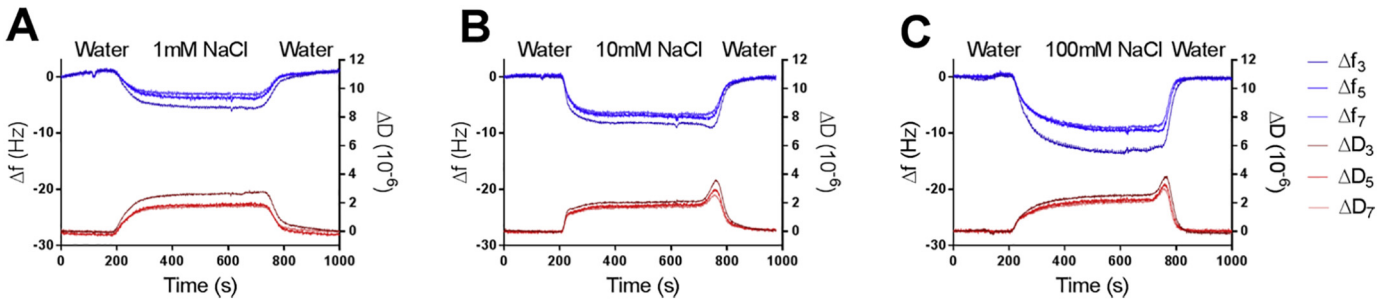


**Fig. 7.** Representative QCM-D curves for grafted LM-B pectin exposed to varying salt concentrations: (A) 1 mM (B) 10 mM (C) 100 mM NaCl.

This echoes to some extent the trends observed for the boundary friction where HM-R showed the lowest friction at low salt concentration and LM-R showed the lowest friction at high salt concentration, albeit with some discrepancies between the ranges of salt concentration at which these effects are observed. Fig. 8B shows the changes in the elastic modulus undergone by the pectin layer under the influence of salt. The difference between the elastic modulus in salt solution and the elastic modulus in water increases for all three pectins up to 50 mM NaCl before decreasing abruptly for higher concentrations. This change also corresponds to an increase in the adsorbed film thickness that indicates a decrease in density of the film and greater fluidity with swelling.

## 4. Discussion

In this study a simple method of fabricating polysaccharide functionalised silicone surfaces is presented. Through a two stage reaction, the grafting of pectin onto PDMS substrates is achieved via its reductive end. The grafted layers are shown to reduce the boundary and mixed friction coefficient compared to bare PDMS. Importantly, the ability of the grafted pectin to enhance lubrication is superior compared to that of the adsorbed pectin and two aspects should be noted. First, the grafted pectin does not require any dissolved pectin in the surrounding media to maintain its lubricating effect, contrarily to adsorbed pectin. This is because the grafted pectin forms a stable layer that cannot desorb or get sheared off from the surface (for the load conditions tested here). Second, the friction coefficient obtained for the grafted pectin is lower than for adsorbed pectin. We hypothesise this effect could be due to the conformation of the pectin: the grafting process “forces” the pectin to stretch out from the surface into an extended (potentially brush-like) conformation whereas the adsorbed pectin adopts flatter configurations that lead to thinner surface films. The brush conformation can better resist interpenetration between the opposite surfaces, thus leading to a lower friction coefficient. In contrast, some studies using end-grafted dextran onto silica did not observe any decrease in the friction coefficient compared to the naked surfaces, unless surfactants were present. This was attributed to the strong (bridging) adhesion between the dextran molecules on the opposing surfaces [41]. In our case, the presence of charges on pectin favour repulsive interactions rather than adhesive forces, thus leading to a decrease in friction.

Biological systems often display sensitivity to solvent conditions. The conformation of proteins and polysaccharides can change upon deviations in pH or ionic strength, which has an impact on their biological functionality. For instance, the mucins composing the salivary film are known to expand or collapse depending on the ionic strength, which changes their lubrication properties [14,15]. Here, we observed a similar effect with the grafted pectin: addition of salt caused a decrease in boundary friction for the three pectins. This is likely a result of the combination of the osmotic resistance to interpenetration displayed by the compressed, counterion-swollen pectin molecules, and the additional hydration lubrication arising from the hydration layers surrounding the sodium counterions [12,63,64]. The three pectins respond differently to the increase in ionic strength despite having similar grafting densities (Table S1). Pectin HM-R, which contains the least amount of charged groups, initially shows a decrease in friction as the ionic strength increases, however this effect tappers off at high ionic strength. We hypothesise that the low number of charges on pectin HM-R causes the amount of counterions that can interact with the charged pectin molecules to reach a limit, which leads to a plateau in the friction coefficient. Pectin LM-R and LM-B have a similar amount of charged groups, however they have different local charge densities: in pectin LM-B, the charges are grouped in “blocks” while in LM-R they are randomly distributed along the molecule. Recent work has highlighted how the blocky character of homogalacturonans (the linear domain of pectin molecule) affects the counter ions condensation on the chains. For a similar DM, homogalacturonans with a blocky character have more ions condensed on the chain than homogalacturonans with randomly distributed charges [65]. Condensed ions are tightly bound to the charged galacturonic acid residue and may therefore play a lesser role in reducing the friction than more loosely associated ions that retain their mobility and own hydration shell. As a result, although both LM-B and LM-R have a similar global charge, the nature of the interaction of the counter-ions with the pectin molecule at the local level is different, which may explain the higher friction measured for LM-B compared to LM-R at high salt concentrations. These findings suggest that in biological systems, such as with the mucins lining mucosal surfaces, lubrication could be modulated by underlying mucosal cells altering either the charge of glycans on the mucins and/or the ionic environment in mucosal fluids.

Unlike in the friction measurements where the grafted pectin is under compression due to the load applied between the ball and the disc, QCM-D allows us to look at the grafted pectin layer under conditions where pectin can swell or contract without mechanical constraints. QCM-D revealed that upon addition of salt, the pectin layer swelled and expanded in a reversible manner. Two response phases are observed in the pectin layer upon addition of salt at varying concentrations. Below 50 mM, the thickness of the pectin layer undergoes only a moderate increase while the increase in the elastic modulus is more pronounced. In this phase, we hypothesise, the counterions can populate the pectin layer without causing the pectin to stretch since at lower concentration they can fill in the voids within the pectin layer. As the ionic strength increases beyond 50 mM, there is not enough space to accommodate all the counterions and their associated water molecules in the pectin layer in its current conformation and the pectin is forced to stretch further and swell under the effect of osmotic pressure. This causes a more pronounced increase in the thickness of the pectin layer as well as a decrease of the elastic modulus due to a reduction in density of the film.

The results here highlight that the hydrated film thickness measured on the QCM-D is not a direct predictor of the boundary friction coefficient. The film thickness of all the pectin films increases with increasing salt concentration above 50 mM. However, the boundary friction coefficient for HM-R and LM-B are relatively constant above salt concentration of 5 mM. In contrast, the boundary friction coefficient for the LM-R pectin film decreases with increasing salt across the whole concentration range and exhibits the lowest friction at high salt. This suggests that the charge distribution is a critical factor for pectin lubrication: the low DM and random distribution of charges on LM-R allows a higher number of ions to interact with the molecule without eliciting ion condensation effects that may manifest in the layers formed by the blocky LM-B. In the absence of counterion condensation, the pectin layers are more effective at attracting more “useful” ions that participate in reducing the friction coefficient through the action of their hydration shells.

Our key innovation is the creation of a soft-elastomeric surface coated in polysaccharides in a brush configuration that is robust enough to withstand the forces present in a tribometer. This mimics the glycosylated macromolecules encountered in biotribological contacts and provides a surface with a chemistry matching those of mucin or lubricin. Our aim has not been to mimic the ultra-low friction associated with these molecules, but to simply provide a polyelectrolyte layer with a biochemical composition relevant to biotribological applications that is responsive to solution environment. With this outcome established, future work should seek to explore factors that influence the conformation and lubrication of the grafted pectin, such as pH or type of counterions (Hofmeister series).

In addition, we anticipate that these pectin-grafted PDMS surfaces have the potential to be suitable for studies concerning food oral tribology. A majority of studies in the field use native PDMS surfaces that are hydrophobic that do not possess surface chemistry akin to the mucosal surface in the mouth [66]. Rendering PDMS hydrophilic is also inappropriate because strategies such oxygen plasma cleaning are only

temporary. The surface of all mucosal epithelial cells is highly decorated with membrane bound mucins that expose their highly hydrated glycosylated brush-like structure to the external environment [67]. Additionally large molecular weight mucins (secretory mucins) are continually extruded and assemble on top of the membrane bound mucins [6,68,69]. We suggest that our pectin-grafted PDMS mimics this membrane-bound hydrated glycosylated 'brush' layer, and is thus a more suitable mimic of the background surface within the oral cavity than bare PDMS substrates. Future work will seek to establish how the various pectins interact with saliva to form a mucosal-mimetic, followed by studies on the interaction of the mucosal-mimetic with food systems.

## 5. Concluding remarks

A new biotribological system has been developed, consisting of covalently end-grafted pectin molecules on a silicone elastomer substrate via an optimised reductive amination process. The grafted pectin layers exhibit lower boundary friction and better resistance to wear than their physically adsorbed counterparts. Increasing the ionic strength of the solution surrounding the grafted pectin caused a decrease in boundary friction and an increase in the hydration and swelling of the pectin layer (to varying degrees depending on the charge density of the pectin). The chemical make-up of the pectin grafted surfaces and the ability to respond to changes in the solvent conditions suggests they could be used as a mimic of biotribological surfaces and provide a more relevant system than the materials conventionally used in the study of biolubrication. In particular, this system could be used to investigate how glycoproteins or polysaccharide present at biointerfaces such as mucins or lubricin respond to specific ions. Importantly, the grafting reaction is very versatile and could be applied to other polysaccharides, making this method a powerful tool to elucidate the fundamentals mechanisms of biolubrication and design superior biomimetic lubricating surfaces for biomedical applications.

In addition, we anticipate that these pectin-grafted PDMS surfaces have the potential to be suitable for studies concerning food oral tribology. A majority of studies in the field use native PDMS surfaces that are hydrophobic that do not possess surface chemistry akin to the mucosal surface in the mouth [66]. Rendering PDMS hydrophilic is also inappropriate because strategies such oxygen plasma cleaning are only temporary. The surface of all mucosal epithelial cells is highly decorated with membrane bound mucins that expose their highly hydrated glycosylated brush-like structure to the external environment [67]. Additionally large molecular weight mucins (secretory mucins) are continually extruded and assemble on top of the membrane bound mucins [6,68,69]. We suggest that our pectin-grafted PDMS mimics this membrane-bound hydrated glycosylated 'brush' layer, and is thus a more suitable mimic of the background surface within the oral cavity than bare PDMS substrates. Future work will seek to establish how the various pectins interact with saliva to form a mucosal-mimetic, followed by studies on the interaction of the mucosal-mimetic with food systems.

## Acknowledgements

This research was funded by the Australian Research Council (DP150104147).

This work was performed in part at the Queensland node of the Australian National Fabrication Facility. A company established under the National Collaborative Research Infrastructure Strategy to provide nano and microfabrication facilities for Australia's researchers.

The authors acknowledge the facilities, and the scientific and technical assistance, of the Australian Microscopy & Microanalysis Research Facility at the Centre for Microscopy and Microanalysis, The University of Queensland, especially Dr. Barry Wood for his help with XPS.

## Appendix A. Supplementary data

Supplementary data to this article can be found online at https://doi.org/10.1016/j.biotri.2019.100092.

## References

[1] W.M. Thomson, H.P. Lawrence, J.M. Broadbent, R. Poulton, The impact of xerostomia on oral-health-related quality of life among younger adults, Health Qual. Life Outcomes 4 (2006) 86.
[2] M. Uchino, D.A. Schaumberg, Dry eye disease: impact on quality of life and vision, Curr. Ophthalmol. Rep. 1 (2) (2013) 51–57.
[3] R.W. Moskowitz, The burden of osteoarthritis: clinical and quality-of-life issues, Am. J. Manag. Care 15 (8 Suppl) (2009) S223–S229.
[4] J. Klein, Molecular mechanisms of synovial joint lubrication, Proc. Inst. Mech. Eng Part J 220 (8) (2006) 691–710.
[5] B. Zappone, M. Ruths, G.W. Greene, G.D. Jay, J.N. Israelachvili, Adsorption, lubrication, and wear of lubricin on model surfaces: polymer brush-like behavior of a glycoprotein, Biophys. J. 92 (5) (2007) 1693–1708.
[6] G.E. Yakubov, H. Gibbins, G.B. Proctor, G.H. Carpenter, Oral mucosa: physiological and physicochemical aspects, Mucoadhesive Materials and Drug Delivery Systems, John Wiley & Sons, Ltd, 2014, pp. 1–38.
[7] G.E. Yakubov, J. McColl, J.H.H. Bongaerts, J.J. Ramsden, Viscous boundary lubrication of hydrophobic surfaces by mucin, Langmuir 25 (4) (2009) 2313–2321.
[8] S. Giasson, N.D. Spencer, Aqueous lubrication with polymer brushes, Aqueous Lubrication, 2014, pp. 183–218.
[9] J. Klein, E. Kumacheva, D. Mahalu, D. Perahia, L.J. Fetters, Reduction of frictional forces between solid surfaces bearing polymer brushes, Nature 370 (6491) (1994) 634–636.
[10] J. Klein, Interactions, friction and lubrication between polymer-bearing surfaces, in: B. Bhushan (Ed.), Fundamentals of Tribology and Bridging the Gap Between the Macro- and Micro/Nanoscales, Springer Netherlands, Dordrecht, 2001, pp. 177–198.
[11] J. Klein, W.H. Briscoe, M. Chen, E. Eiser, N. Kampf, U. Raviv, R. Tadmor, L. Tsarkova, Polymer brushes and surface forces, Polymer Adhesion, Friction, and Lubrication, John Wiley & Sons, Inc, 2013, pp. 135–176.
[12] J. Klein, Hydration lubrication, Friction 1 (1) (2013) 1–23.
[13] S. Lee, N.D. Spencer, Sweet, hairy, soft, and slippery, Science 319 (5863) (2008) 575–576.
[14] L. Macakova, G.E. Yakubov, M.A. Plunkett, J.R. Stokes, Influence of ionic strength changes on the structure of pre-adsorbed salivary films. A response of a natural multi-component layer, Colloids Surf. B: Biointerfaces 77 (1) (2010) 31–39.
[15] L. Macakova, G.E. Yakubov, M.A. Plunkett, J.R. Stokes, Influence of ionic strength on the tribological properties of pre-adsorbed salivary films, Tribol. Int. 44 (9) (2011) 956–962.
[16] S. Lee, N.D. Spencer, Adsorption properties of poly(L-lysine)-graft-poly(ethylene glycol) (PLL-g-PEG) at a hydrophobic Interface: influence of tribological stress, pH, salt concentration, and polymer molecular weight, Langmuir 24 (17) (2008) 9479–9488.
[17] S.S. Perry, X. Yan, F.T. Limpoco, S. Lee, M. Müller, N.D. Spencer, Tribological properties of poly(l-lysine)-graft-poly(ethylene glycol) films: influence of polymer architecture and adsorbed conformation, ACS Appl. Mater. Interfaces 1 (6) (2009) 1224–1230.
[18] S.N. Ramakrishna, R.M. Espinosa-Marzal, V.V. Naik, P.C. Nalam, N.D. Spencer, Adhesion and friction properties of polymer brushes on rough surfaces: a gradient approach, Langmuir 29 (49) (2013) 15251–15259.
[19] P. Nalam, J. Clasohm, A. Mashaghi, N. Spencer, Macrotribological studies of poly(L-lysine)-graft-poly(ethylene glycol) in aqueous glycerol mixtures, Tribol. Lett. 37 (3) (2010) 541–552.
[20] P.C. Nalam, S.N. Ramakrishna, R.M. Espinosa-Marzal, N.D. Spencer, Exploring lubrication regimes at the nanoscale: nanotribological characterization of silica and polymer brushes in viscous solvents, Langmuir 29 (32) (2013) 10149–10158.
[21] M.T. Müller, X. Yan, S. Lee, S.S. Perry, N.D. Spencer, Preferential solvation and its effect on the lubrication properties of a surface-bound, Brushlike copolymer, Macromolecules 38 (9) (2005) 3861–3866.
[22] M.T. Müller, X. Yan, S. Lee, S.S. Perry, N.D. Spencer, Lubrication properties of a Brushlike copolymer as a function of the amount of solvent absorbed within the brush, Macromolecules 38 (13) (2005) 5706–5713.
[23] S. Lee, M. Müller, M. Ratoi-Salagean, J. Vörös, S. Pasche, S. De Paul, H. Spikes, M. Textor, N. Spencer, Boundary lubrication of oxide surfaces by poly(L-lysine)-g-poly(ethylene glycol) (PLL-g-PEG) in aqueous media, Tribol. Lett. 15 (3) (2003) 231–239.
[24] C. Perrino, S. Lee, N. Spencer, End-grafted sugar chains as aqueous lubricant additives: synthesis and macrotribological tests of poly(l-lysine)-graft-dextran (PLL-g-dex) copolymers, Tribol. Lett. 33 (2) (2009) 83–96.
[25] K.J. Rosenberg, T. Goren, R. Crockett, N.D. Spencer, Load-induced transitions in the lubricity of adsorbed poly(L-lysine)-g-dextran as a function of polysaccharide chain density, ACS Appl. Mater. Interfaces 3 (8) (2011) 3020–3025.
[26] M. Chen, W.H. Briscoe, S.P. Armes, J. Klein, Lubrication at physiological pressures by polyzwitterionic brushes, Science 323 (5922) (2009) 1698–1701.
[27] O. Tairy, N. Kampf, M.J. Driver, S.P. Armes, J. Klein, Dense, highly hydrated

polymer brushes via modified atom-transfer-radical-polymerization: structure, surface interactions, and frictional dissipation, Macromolecules 48 (1) (2015) 140–151.
[28] M. Chen, W.H. Briscoe, S.P. Armes, H. Cohen, J. Klein, Polyzwitterionic brushes: extreme lubrication by design, Eur. Polym. J. 47 (4) (2011) 511–523.
[29] M.F. Maitz, Applications of synthetic polymers in clinical medicine, Biosurf. Biotribol. 1 (3) (2015) 161–176.
[30] S. Lee, M. Müller, K. Rezwan, N.D. Spencer, Porcine gastric mucin (PGM) at the water/poly(dimethylsiloxane) (PDMS) interface: influence of pH and ionic strength on its conformation, adsorption, and aqueous lubrication properties, Langmuir 21 (18) (2005) 8344–8353.
[31] T. Crouzier, K. Boettcher, A.R. Geonnotti, N.L. Kavanaugh, J.B. Hirsch, K. Ribbeck, O. Lieleg, Modulating mucin hydration and lubrication by deglycosylation and polyethylene glycol binding, Adv. Mater. Interfaces 2 (18) (2015) 1500308.
[32] J.B. Madsen, J. Sotres, K.I. Pakkanen, P. Efler, B. Svensson, M. Abou Hachem, T. Arnebrant, S. Lee, Structural and mechanical properties of thin films of bovine submaxillary mucin versus porcine gastric mucin on a hydrophobic surface in aqueous solutions, Langmuir 32 (38) (2016) 9687–9696.
[33] N.M. Harvey, G.E. Yakubov, J.R. Stokes, J. Klein, Normal and shear forces between surfaces bearing porcine gastric mucin, a high-molecular-weight glycoprotein, Biomacromolecules 12 (4) (2011) 1041–1050.
[34] B. Zappone, G.W. Greene, E. Oroudjev, G.D. Jay, J.N. Israelachvili, Molecular aspects of boundary lubrication by human lubricin: effect of disulfide bonds and enzymatic digestion†, Langmuir 24 (4) (2008) 1495–1508.
[35] V.J. Schomig, B.T. Kasdorf, C. Scholz, K. Bidmon, O. Lieleg, S. Berensmeier, An optimized purification process for porcine gastric mucin with preservation of its native functional properties, RSC Adv. 6 (50) (2016) 44932–44943.
[36] O. Sterner, C. Karageorgaki, M. Zürcher, S. Zürcher, C.W. Scales, Z. Fadli, N.D. Spencer, S.G.P. Tosatti, Reducing friction in the eye: a comparative study of lubrication by surface-anchored synthetic and natural ocular mucin analogues, ACS Appl. Mater. Interfaces 9 (23) (2017) 20150–20160.
[37] A. Singh, M. Corvelli, S.A. Unterman, K.A. Wepasnick, P. McDonnell, J.H. Elisseeff, Enhanced lubrication on tissue and biomaterial surfaces through peptide-mediated binding of hyaluronic acid, Nat. Mater. 13 (2014) 988.
[38] D.W. Lee, X. Banquy, S. Das, N. Cadirov, G. Jay, J. Israelachvili, Effects of molecular weight of grafted hyaluronic acid on wear initiation, Acta Biomater. 10 (5) (2014) 1817–1823.
[39] M. Benz, N. Chen, J. Israelachvili, Lubrication and wear properties of grafted polyelectrolytes, hyaluronan and hylan, measured in the surface forces apparatus, J. Biomed. Mater. Res. Part A 71A (1) (2004) 6–15.
[40] J. Yu, X. Banquy, G.W. Greene, D.D. Lowrey, J.N. Israelachvili, The boundary lubrication of chemically grafted and cross-linked hyaluronic acid in phosphate buffered saline and lipid solutions measured by the surface forces apparatus, Langmuir 28 (4) (2012) 2244–2250.
[41] C.E. McNamee, S. Yamamoto, M. Kappl, H.-J. Butt, K. Higashitani, A. Dėdinaitė, P.M. Claesson, Surface and friction forces between grafted polysaccharide layers in the absence and presence of surfactant, J. Colloid Interface Sci. 364 (2) (2011) 351–358.
[42] T. Goren, N.D. Spencer, R. Crockett, Impact of chain morphology on the lubricity of surface-grafted polysaccharides, RSC Adv. 4 (41) (2014) 21497–21503.
[43] J. Chen, W. Liu, C.-M. Liu, T. Li, R.-H. Liang, S.-J. Luo, Pectin modifications: a review, Crit. Rev. Food Sci. Nutr. 55 (12) (2015) 1684–1698.
[44] J.R. Stokes, L. Macakova, A. Chojnicka-Paszun, C.G. de Kruif, H.H.J. de Jongh, Lubrication, adsorption, and rheology of aqueous polysaccharide solutions, Langmuir 27 (7) (2011) 3474–3484.
[45] A. Ström, P. Ribelles, L. Lundin, I. Norton, E.R. Morris, M.A.K. Williams, Influence of pectin fine structure on the mechanical properties of calcium – pectin and acid – pectin gels, Biomacromolecules 8 (9) (2007) 2668–2674.
[46] M.-C. Ralet, V. Dronnet, H.C. Buchholt, J.-F. Thibault, Enzymatically and chemically de-esterified lime pectins: characterisation, polyelectrolyte behaviour and calcium binding properties, Carbohydr. Res. 336 (2) (2001) 117–125.
[47] J.H.H. Bongaerts, K. Fourtouni, J.R. Stokes, Soft-tribology: lubrication in a compliant PDMS-PDMS contact, Tribol. Int. 40 (2007) 1531–1542 10-12 SPEC. ISS.
[48] NIST X-ray Photoelectron Spectroscopy Database, Version 4.1, National Institute of Standards and Technology, Gaithersburg, 2012.
[49] R.J. Moore, J.T.F. Watts, J.A.A. Hood, D.J. Burritt, Intra-oral temperature variation over 24 hours, Eur. J. Orthodontics 21 (3) (1999) 249.
[50] N. Efron, G. Young, N.A. Brennan, Ocular surface temperature, Curr. Eye Res. 8 (9) (1989) 901–906.
[51] M. Sniegowski, M. Erlanger, R. Velez-Montoya, J.L. Olson, Difference in ocular surface temperature by infrared thermography in phakic and pseudophakic patients, Clin. Ophthalmol. 9 (2015) 461–466.
[52] H. Fujiwara, Data Analysis, in: J.W. Sons (Ed.), Spectroscopic Ellipsometry : Principles and Applications, 2007.
[53] K. Nikolova, I. Panchev, S. Sainov, Optical characteristics of biopolymer films from pectin and gelatin, J. Optoelectron. Adv. Mater. 7 (3) (2005) 1439–1444.
[54] C. Pradal, P. Kithva, D. Martin, M. Trau, L. Grondahl, Improvement of the wet tensile properties of nanostructured hydroxyapatite and chitosan biocomposite films through hydrophobic modification, J. Mater. Chem. 21 (7) (2011) 2330–2337.
[55] J.S. Stevens, S.L.M. Schroeder, Quantitative analysis of saccharides by X-ray photoelectron spectroscopy, Surf. Interface Anal. 41 (6) (2009) 453–462.
[56] X. Cao, M.E. Pettit, S.L. Conlan, W. Wagner, A.D. Ho, A.S. Clare, J.A. Callow, M.E. Callow, M. Grunze, A. Rosenhahn, Resistance of polysaccharide coatings to proteins, hematopoietic cells, and marine organisms, Biomacromolecules 10 (4) (2009) 907–915.
[57] M. Biesalski, J. Rühe, Scaling laws for the swelling of neutral and charged polymer brushes in good solvents, Macromolecules 35 (2) (2002) 499–507.
[58] L. Salbu, A. Bauer-Brandl, I. Tho, Direct compression behavior of low- and high-methoxylated pectins, AAPS PharmSciTech 11 (1) (2010) 18–26.
[59] B. Lego, W.G. Skene, S. Giasson, Swelling study of responsive polyelectrolyte brushes grafted from mica substrates: effect of pH, salt, and grafting density, Macromolecules 43 (9) (2010) 4384–4393.
[60] J. Cybulska, A. Brzyska, A. Zdunek, K. Woliński, Simulation of force spectroscopy experiments on galacturonic acid oligomers, PLoS One 9 (9) (2014) e107896.
[61] S.M. Bhattacharjee, G.A. Achille, A. Maritan, Flory theory for polymers, J. Phys. Condens. Matter 25 (50) (2013) 503101.
[62] W.J. Brittain, S. Minko, A structural definition of polymer brushes, J. Polym. Sci. A Polym. Chem. 45 (16) (2007) 3505–3512.
[63] U. Raviv, S. Giasson, N. Kampf, J.-F. Gohy, R. Jerome, J. Klein, Lubrication by charged polymers, Nature 425 (6954) (2003) 163–165.
[64] U. Raviv, S. Giasson, N. Kampf, J.-F. Gohy, R. Jérôme, J. Klein, Normal and frictional forces between surfaces bearing polyelectrolyte brushes, Langmuir 24 (16) (2008) 8678–8687.
[65] A.H. Irani, J.L. Owen, D. Mercadante, M.A.K. Williams, Molecular dynamics simulations illuminate the role of counterion condensation in the electrophoretic transport of homogalacturonans, Biomacromolecules 18 (2) (2017) 505–516.
[66] C. Pradal, J.R. Stokes, Oral tribology: bridging the gap between physical measurements and sensory experience, Curr. Opin. Food Sci. 9 (2016) 34–41.
[67] M.E.V. Johansson, H. Sjövall, G.C. Hansson, The gastrointestinal mucus system in health and disease, Nat. Rev. Gastroenterol. Hepatol. 10 (2013) 352.
[68] P. Roussel, P. Delmotte, The diversity of epithelial secreted mucins, Curr. Org. Chem. 8 (5) (2004) 413–437.
[69] D.J. Thornton, K. Rousseau, M.A. McGuckin, Structure and function of the polymeric mucins in airways mucus, Annu. Rev. Physiol. 70 (1) (2008) 459–486.